Small-Angle Neutron Scattering, Electron Paramagnetic Resonance, Electrophoretic NMR, and Time-Resolved Fluorescence Quenching Studies of Sodium Dodecyl Sulfate and Tetra(ethylene oxide) Dodecyl Ether Mixed Surfactant Micelles

P. C. Griffiths,* A. Y. F. Cheung, C. Farley, and A. Paul

School of Chemistry, Cardiff University, P.O. Box 912, Cardiff CF10 3TB, U.K.

R. K. Heenan and S. M. King

ISIS Facility, Rutherford Appleton Laboratory, Chilton, Didcot OX11 OQX, U.K.

E. Pettersson and P. Stilbs

Physical Chemistry, Royal Institute of Technology, Stockholm S-100 44, Sweden

Radha Ranganathan

Department of Physics and Astronomy and the Center for Supramolecular Studies. California State University, Northridge, California 91330-8268

Received: May 9, 2003; In Final Form: November 25, 2003

Small-angle neutron scattering (SANS), time-resolved fluorescence quenching (TRFQ), electrophoretic NMR (ENMR), and electron paramagnetic resonance (EPR) have been used to study mixed micelles formed from the two dodecyl tailed surfactants, sodium dodecyl sulfate (SDS) and tetra(ethylene oxide) dodecyl ether. By combining the TRFQ and EPR techniques, one is essentially able to calculate the SANS data, lending significant weight to the micelle characteristics thus obtained. EPR reports the degree of hydration of the surfactant headgroups; TRFQ, the micelle aggregation number and inter alia the volume of the hydrophobic core. Given the physical dimensions of the surfactant, i.e., alkyl chain length, headgroup volumes, etc., it is then possible to calculate the micelle ellipticity and shell thickness. The ENMR studies provide a rather different but complementary estimate of the ionic character of the micelle. With increasing nonionic content, the aggregation number increases, the micelle becomes more elliptical, and the headgroup region of the micelle becomes less hydrated and significantly more viscous. The degree of sodium counterion dissociation shows an initial small decrease with decreasing SDS micelle mole fraction but subsequently increases, reflecting the interplay between the electrostatic character of the micelle surface and the micelle curvature.

Introduction

Surfactant mixtures are encountered everyday in numerous technological, domestic, and industrial applications. The mixture may arise inherently due to structural heterogeneity or purposely because blending surfactants often improve the formulation performance or cost-effectiveness. However, the properties of the mixed surfactant system are invariably quite different from those of the two individual components. Understanding the origins of this nonideality is therefore important for both fundamental and application-related reasons.[1]

Considerable attention in the literature has focused on developing theories to describe the onset of micellization and the composition of the mixed surfactant micelles formed. The most commonly used approaches are (i) the ideal mixing model of Clint,[2] which has been quite successful in describing mixed systems of similar surfactants; (ii) Rubingh's[3] very successful, but largely empirical, regular solution theory (RST) centered on the parameter β to account for specific interactions between the two surfactants; and (iii) the more comprehensive molecular-thermodynamic models of Blankschtein et al.[4,5] and Bergstrom et al.[6]

A significant number of studies also consider the morphology of mixed surfactant micelles, and scattering techniques have played a pivotal role in this regard. Arguably the most appropriate technique is that of small-angle neutron scattering.[7,8] SANS is a very powerful technique for studying the morphology (size and shape) of the structures formed in aqueous solution by surfactants, as well as the interaction between them, but usually within the context of a particular model. To obtain the most physically reasonable model, it is important to seek other experimental information. One approach is to use fluorescence quenching to determine the aggregation number of the micelle.[10] To this end, when fitting small-angle neutron scattering (SANS) data, we use the micelle aggregation number extracted from time-resolved fluorescence quenching (TRFQ) and an estimate of the amount of water in the polar shell of the micelle comprising the solvated headgroups derived from electron paramagnetic resonance (EPR). From the aggregation number one may calculate the volume of the hydrophobic core. From a knowledge of the length of the alkyl tail, and thus the micelle radius, it is then possible to calculate the ellipticity of the micelle. This approach is particularly advantageous as the SANS fitting is insensitive to the ellipticity. Unrestricted, it is virtually impossible to fit the amount of water in the polar shell to any degree of satisfaction. Limiting this value is therefore highly desirable.

10.1021/jp035276i CCC: $27.50
Published on Web 12/31/2003

Our recent SANS/EPR/TRFQ studies have focused on binary mixtures of the anionic surfactant sodium dodecyl sulfate (SDS) and a series of sugar-based nonionic surfactants, *n*-alkylmalonobis(*N*-methylglucamide)s (C_nBNMG),[9−14] but that work is complicated by the fact that the large number of hydroxyl groups (−OH) on the sugar cannot be distinguished from hydration water in the EPR analysis. Accordingly, a somewhat simpler nonionic surfactant is required. $C_{12}E_4$, with only a single terminal −OH group, has therefore been employed. Further, SDS/$C_{12}E_4$ mixtures have been studied previously by a range of different but complementary techniques (surface tension, fluorescence quenching and ζ-potential,[15] static fluorescence and electrical conductivity[16]), and thus this system is an ideal one on which to base our SANS/EPR/TRFQ approach. Similarly, closely analogous systems have also been studied by SANS (SDS/$C_{12}E_m$, where $m = 6$;[17,18] sodium dodecylsulfonate (SDOS)/$C_{12}E_m$, where $m = 6$[19]), light scattering (SDS/$C_{12}E_m$, where $m = 6$[20] and $m = 5$[21]), EPR (SDS/$C_{12}E_m$, where $m = 6$[42]), and surfactant-selective electrodes (SDS/$C_{12}E_m$, where $m = 6$[22]).

Experimental Section

Materials. Tetra(ethlyene oxide) dodecyl ether $C_{12}E_4$ (Aldrich) was used as received. Sodium dodecyl sulfate (Aldrich) was recrystallized from ethanol until no dip in the surface tension−concentration plot could be detected around the CMC. The perdeuterated SDS (Aldrich) was not recrystallized prior to use but should not affect the results given the relatively high concentration at which it was used. All other reagents were of analytical grade and used as received. The solvent was D_2O and H_2O in the SANS and EPR measurements, respectively. Throughout this work, measurements were made at a total surfactant concentration of 50 mM, with the exception of pure SDS, which was measured at 25 mM on a separate occasion.

Time-Resolved Fluorescence Quenching (TRFQ). TRFQ measurements were carried out with pyrene as the probe and dimethylbenzophenone as the quencher (Aldrich, used as received). The samples were all prepared from one mother solution in a manner that allowed the relative values of the quencher/surfactant molar ratios to be determined with high precision. The average number of quenchers per micelle, was maintained constant, avoiding systematic errors that sometimes plague the interpretation of TRFQ data. The fluorescence decay curves of pyrene were obtained at 25 °C using an FL900 lifetime spectrometer (Edinburgh Analytical Instruments) and fit to the Infelta-Tachiya model[23−25] using the software provided by the manufacturer. Before fitting, the decay curves were corrected for the instrument response. Details of the experimental setup and the procedure for calculating values of aggregation numer are identical to those previously reported.[26]

Small-Angle Neutron Scattering. The SANS measurements were performed as detailed previously[11] on the fixed-geometry, time-of-flight LOQ diffractometer (ISIS Spallation Neutron Source, Oxfordshire, U.K.). All measurements were carried out at 25 °C. Experimental measuring times were between 40 and 80 min. All scattering data were normalized for the sample transmission and incident wavelength distribution, corrected for instrumental and sample backgrounds using an empty quartz cell, and for the linearity and efficiency of the detector response. The data were put onto an absolute scale using a well-characterized partially deuterated polystyrene-blend standard sample.

SANS Data Fitting and Analysis. For globular micelles, the analytical procedure for quantifying micelle structure from SANS data is that developed by Hayter and Penfold.[27] For a solution of interacting charged micelles, the intensity of scattered radiation, $I(Q)$, as a function of the wave-vector, Q, is given by

$$I_{\text{surfac}tant}(Q) = n[S(Q)\langle|F(Q)|^2\rangle + |\langle F(Q)\rangle|^2 - \langle|F(Q)|^2\rangle] + B_{\text{inc}} \quad (1)$$

where $F(Q) = V_1(\rho_1 - \rho_2)F_0(QR_1) + V_2(\rho_2 - \rho_0)F_0(QR_2)$. The first term represents the scattering from the hydrocarbon core (subscript 1) and the second, the polar shell (subscript 2). $V_i = 4/3\pi R_i^3$ and $F_0(QR)3j_i(QR)/QR$ (j_i is the first-order spherical Bessel function). $S(Q)$ represents the spatial arrangement of the micelles in solution, and n, the micelle number density. Equation 1 invokes the "decoupling approximation"; i.e., there is no correlation between the position of the micelle and its orientation.[7] ρ_i is the neutron scattering length density of the micellar core (subscript 1), the polar shell (subscript 2), and the solvent (subscript 0). These constants are combined into a single fittable parameter used to "scale" the model intensity to the absolute value. Postfitting, this scalar is recalculated using the parameters describing the micelle morphology/composition and the molar concentration of micelles to validate the fit. The calculated and observed values should lie within ∼10%.

To calculate the various parameters required to setup the SANS fitting approach, the micelle composition, usually expressed as the micelle mole fraction of SDS (x_{SDS}) is required. We have followed the elegant method of Penfold et al.[17] using parallel molar ratios of $C_{12}E_4$/protonated-SDS and $C_{12}E_4$/deuterated-SDS to extract x_{SDS}. For brevity, these results are not presented here because in all cases the micelle mole fraction was equal to the solution mole fraction within experimental error. This observation is in excellent agreement with that of Penfold et al,[17] who showed that the same behavior occurred in their SDS/$C_{12}E_6$ system as low as 10 mM. All data are nonetheless expressed as SDS micelle mole fraction x_{SDS}. It is important to note, however, that the composition of a micelle thus obtained is **model-independent**—it does not rely on any fitting of the data.

The model of the micelle adopted here is that of a charged particle with an elliptical core−shell morphology. In the ellipsoid model the average volume per headgroup and average scattering length density of the dry surfactant headgroup are input as **constants**, calculated from the composition of the micelle and the values for the respective dry headgroup volumes. Modeling of the structure of the anionic surfactant headgroup is complicated by the sodium counterion dissociation α_{Na^+} which is required to calculate the corresponding ρ_{SDShead} and volume. However, in practice the headgroup scattering length density and volume are not that sensitive to this parameter; for $\alpha_{Na^+} = 0.27$ (i.e., pure SDS), $\rho_{\text{SDShead}} = 3.30 \times 10^{-6}$ Å^{-2} and volume 70.5 Å^3, whereas for $\alpha_{Na^+} = 0.5$, $\rho_{\text{SDShead}} = 3.45 \times 10^{-6}$ Å^{-2} and volume 67.5 Å^3. The dissociation does, however, significantly affect the charge on the micelle and hence the structure factor $S(Q)$, a point we return to later in the discussion. For the tetra(ethylene oxide), $\rho_{\text{EOhead}} = 0.48 \times 10^{-6}$ Å^{-2} and volume 265 Å^3. The core scattering length density is also taken to be constant, i.e., independent of x_{SDS}, with a value corresponding to dodecane. The volume of the hydrophobic core is calculated from the volume of the dodecyl tail ($V_{\text{tail}} = 353$ Å^3) scaled by the aggregation number, N_{agg} (Table 1), and because $R_{\text{dodecyl}} = 16.7$ Å, the axial ratio $X = 3V_{\text{tail}}N_{\text{agg}}/4\pi R_{\text{dodecyl}}^3$. For all the data here this was found to be the optimum value.

To illustrate the insensitivity of SANS to the headgroup region, consider a shell region comprising a number of headgroups and associated water such that the average shell scattering

TABLE 1: Sodium Dodecyl Sulfate SDS/Tetra(ethylene oxide) Dodecyl Ether SANS Analysis, Constrained Core−Shell Fit[a]

x_{SDS}	aggregation no. ± 3	δ_{shell}/Å ± 0.1	R_{core}/Å ± 0.1	axial ratio ± 0.1	α_{Na^+} ± 0.05
1.00	65	3.6	16.7	1.2	n/a
0.95	85	3.7	16.7	1.5	0.27
0.90	88	3.8	16.7	1.6	0.28
0.85	91	3.9	16.7	1.6(5)	0.29
0.80	95	4.2	16.7	1.7	0.29

[a] δ_{shell}, R_{core}, and axial ratio are all constrained from the aggregation number.

TABLE 2: SANS and ENMR Estimates of the Degree of Sodium Counterion Dissociation for Sodium Dodecyl Sulfate SDS/Tetra(ethylene oxide) Dodecyl Ether Micelles

x_{SDS}	large particle limit α_{Na^+} ± 0.05	SANS α_{Na^+} ± 0.05
1.00	0.27	0.27
0.95	0.22	0.27
0.90	0.24	0.28
0.85	0.26	0.29
0.80	0.27	0.29

length density is given by $\bar{\rho} = \phi_{water}\rho_{water} + (1 - \phi_{water})\bar{\rho}_{headgroups}$. Because $\phi_{water} = V_{water}/V_{shell}$, the parameters V_{water} and V_{shell} are strongly coupled and not amenable to fitting. We adopt the approach of fixing ϕ_{water} at the EPR determined value that, inter alia, defines the shell volume (thickness). The scattering length density of the hydrated shell region is then (re)calculated within the analysis software, on the basis of ϕ_{water}. Hence, constraining this value eliminates the trial-and-error aspects required in previous work to find the overall "best fit" value of ϕ_{water} due to local minima in the least-squares fits.[28]

The structure factor $S(Q)$ was calculated using the Hayter and Penfold model[29] for spheres of a given micellar concentration, charge, and ionic strength, incorporating refinements for low volume fractions and a penetrating ionic background. Various approaches to parametrizing the structure factor were adopted on the basis of known or measured estimates of the micelle size, surfactant concentration, and the degree of sodium counterion binding to calculate the hard-sphere volume fraction, charge, and Debye length. We have shown[30] that this method of calculating the structure factor, which assumes spherical particles, remains valid for dilute, isotropic samples of micelles with small degrees of ellipticity, as is the case here.

Electron Paramagnetic Resonance. Experimental details for the EPR measurements are also identical to those described previously,[10] and only brief details are repeated here. Stock solutions of the two surfactants with spin-probe/surfactant molar ratios of 1/400 were mixed to yield the desired solution composition. These nondegassed samples were sealed with a gas-oxygen torch into melting point capillaries, which were housed within a quartz EPR tube for the measurements. The temperature was controlled to ±0.2 K by a Bruker variable temperature unit BVT 2000. Five spectra were taken at X-band on a Bruker ESP-300 spectrometer.

EPR Line Shape Fitting and Analysis. The line shapes were fitted to a Voigt approximation to separate the Gaussian and Lorentzian components of the spectral lines and to locate the resonance fields of the three EPR lines of a nitroxide radical to a precision of a few milligauss. Rotational correlation times are computed from the overall line width of the center line and the peak-to-peak heights of the three lines and corrected for inhomogeneous broadening using the procedure outlined by Bales.[31,32]

The separation A+ of the low and center lines ($M_I = +1$ and $M_I = 0$) is directly related to the polarity index H(25°C), defined as the molar ratio of OH groups in a given volume relative to water. For simple SDS solutions, H(25°C) corresponds to the volume fraction of water in the polar shell, ϕ_{water}. In the previous work on SDS/sugar surfactant mixtures,[10,12] the majority of the 10 sugar −OH groups per nonionic surfactant contributed to H(25°C) and therefore the EPR results could not be used to constrain the SANS fitting. For the data presented in this Article, this problem is minimized and the EPR results can be used to validate the combined EPR−SANS approach.

Electrophoretic NMR. In the presence of an electric field, charged micelles attain a drift velocity $u_{\pm}$, which is superimposed upon their random diffusional motion. The diffusional mobility is far greater ($\sim 10^2$ m^2 s^{-1}) than the mobility induced by an electric field ($10^{-4}-10^{-6}$ m^2 s^{-1}). Classical methods for measuring counterion binding (e.g., conductivity) cannot be applied to mixed surfactant systems as the micelle composition changes with dilution and the conductivity is dominated by the counterions, which are much more mobile. To determine the mobility of the larger, micellar species, we use pulsed-gradient spin−echo PGSE-NMR. A further advantage of the NMR technique is the ability to follow the behavior of each chemically distinct component in the mixture in a single measurement.

The electrophoretic nuclear magnetic resonance (ENMR) technique was conceived by Holtz et al.[33,34] and subsequently developed by Johnson[35−37] and others.[38,39] Measurements were conducted on a Bruker AMX300 NMR spectrometer using a custom-designed glass U-tube of 2 mm outside diameter coated with polyacrylamide to reduce electro-osmosis.[40] The arrangement is held securely in the center of the active volume of a 10 mm diffusion probe (Cryomagnet Systems, Indianapolis, IN). A constant current pulsed electric field generator designed by S. Woodward (University of North Carolina, Chapel Hill, NC) was used to deliver the current to two platinum wires extending just below the liquid surfaces.

The displacement induced by the electric field, typically 20 μm, was quantified using the spatial resolution of a simple form of NMR imaging, on the basis of the attenuation of the spin−echo caused by the molecules experiencing different "read" and "write" field gradient pulses. Whereas the random diffusional motion of the surfactants results in an exponentially damped attenuation, the coherent motion induced by the electric field results in a phase shift of the spin−echo given by

$$I(G,\delta,\Delta,\nu) = I_o \cos(\gamma G\delta\nu\Delta) \exp\left[-\gamma^2\delta^2G^2\left(\Delta - \frac{\delta}{3}\right)D_s\right] \quad (2)$$

where I is the integral of the relaxation-weighted Fourier transformed peak intensity in the absence (I_0) and presence ($I(G,\delta,\Delta,\nu)$) of flow and field gradients. The exponential term accounts for the attenuation due to diffusion. To maximize the electric field induced displacements with manageable pulsed electric fields, a diffusion time (Δ) of 0.5 s was used, which necessitated a stimulated echo sequence with $\tau = 10$ ms. The attenuation of the signal due to relaxation was therefore kept to a minimum and was approximately 30%. Typically, gradient pulses were 1 ms in duration (δ) with intensity (G) 0.44 T/m.

Results and Discussion

The TRFQ-derived aggregation numbers are presented in Table 1. These values are in excellent agreement with the TRFQ results of Iglesias and Montenegro[16] and Gehlen et al.[15] on the same systems, and the SANS results of Penfold et al.[17] who report $N_{agg} \sim 90$ for the related system SDS/$C_{12}E_6$/0.1 M NaCl.

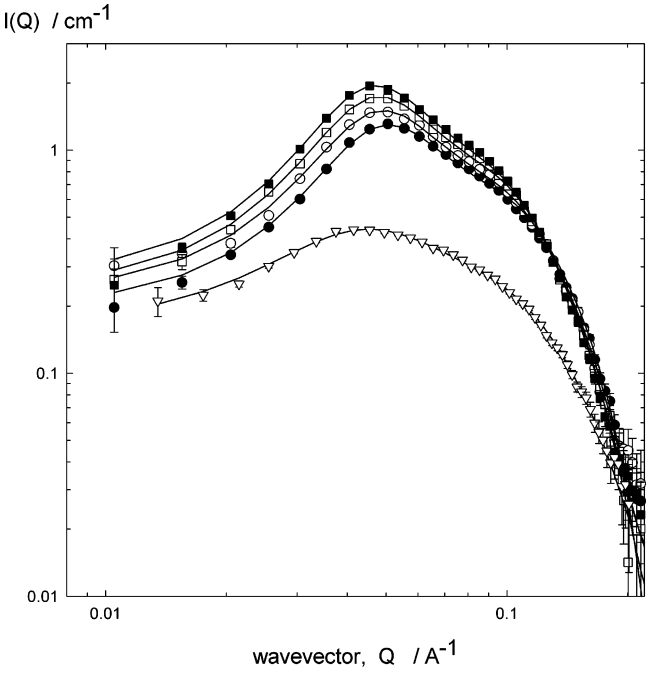

Figure 1. Intensity of scattered radiation as a function of wavevector, Q (linear-linear representation), for binary surfactant micelles comprising SDS and $C_{12}E_4$ in D_2O. (■) $\alpha_{SDS} = 1.0$ (25 mM); (●) $\alpha_{SDS} = 0.95$ (50 mM); (○) $\alpha_{SDS} = 0.90$ (50 mM); (□) $\alpha_{SDS} = 0.85$ (50 mM); (▽) $\alpha_{SDS} = 0.80$ (50 mM). The solid lines drawn through the data points correspond to the fits to the constrained model as described in the test.

The slight growth in ellipticity is also in good agreement with the hydrodynamic behavior of Brown et al.[21] in their light scattering study on SDS/$C_{12}E_5$.

The scattering profiles of all the binary surfactant mixtures are shown in Figure 1. The parameters defining the fits are given in Table 1. There are clear differences in the various data sets, with the increase in intensity with decreasing x_{SDS} principally due to a combination of the reduction in the charge on the micelle and the increasing number of scattering bodies (associated with the decreasing critical micelle concentration). The radius of the micelle, R_{core}, the shell thickness δ_{shell}, and axial ratio are all constrained as described above given the value of the aggregation number, N_{agg}. However, allowing these to float freely resulted in values that did not vary more that 10% from the initial estimates. Thus, TRFQ can indeed be used to constrain the overall size and shape of the surfactant micelle when SANS data are fitted; any differences observed in the estimates of N_{agg} from different techniques/laboratories is a reflection of the model used.[30] This permits a closer inspection of the detail, such as the degree of hydration of the surfactant headgroups.

The volume fraction of water in the polar shell ϕ_{water} (equivalent to the polarity index H(25°C)) may be calculated from the hyperfine coupling constant in an EPR experiment. These data are shown in Figure 2 as a function of SDS micelle mole fraction x_{SDS}. ϕ_{water} increases with increasing x_{SDS} because the anionic headgroup is smaller ($V_{headgroup} = 70.5$ Å^3) than the nonionic ($V_{headgroup} = 265$ Å^3), permitting a greater degree of water penetration into the headgroup region. Indeed, the fits in Figure 1 have been constrained such that the degree of hydration of the surfactant headgroups is identical to the EPR value, lending considerable weight to the validity of the three techniques.

The lessening degree of hydration with increasing nonionic mole fraction exhibited here is consistent with all our other EPR & SANS studies on SDS/sugar surfactants.[12,41] It is, however,

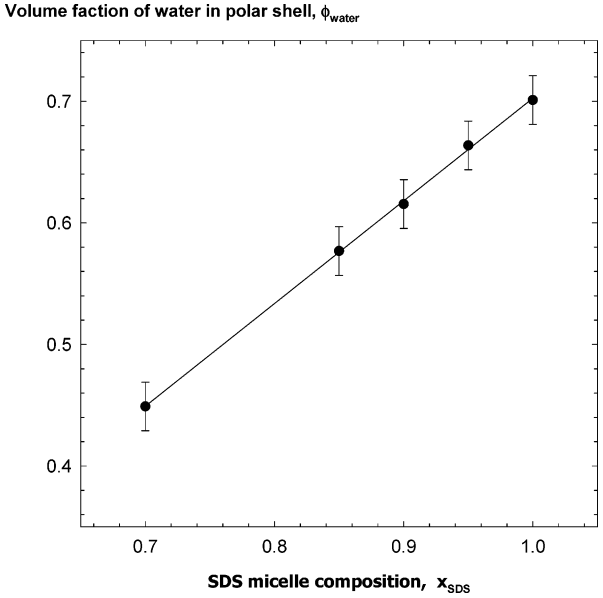

Figure 2. Polar shell water volume fraction ϕ_{water} calculated from the EPR-derived polarity A+ of mixed micelles comprising sodium dodecylsulfate SDS and $C_{12}E_4$ as a function of micelle composition x_{SDS}.

different from the earlier work of Baglioni et al.[42] that show the degree of hydration for a related system SDS/$C_{12}E_6$ going through a maximum at $x_{SDS} = 0.5$. That work, however, used a different spin-probe (*x*-doxylstearic acids) and selectively deuterated surfactants. Conversely, and in agreement with our data, is the conclusion drawn by Gehlen et al.[23] and Iglesias and Montenegro[16] from fluorescence studies using micelle solubilized pyrene. The polarity, as indicated by the I_1/I_3 ratio, decreases gradually on addition of $C_{12}E_4$ to SDS solutions. When Triton 100, a large nonionic commercial surfactant, is added to SDS solutions, the opposite is observed[43] and is thought to arise due to probe relocation associated with the increase in micelle size.

A manifestation of the effects of the expulsion of water from the headgroup region can be obtained from the mobility of a micelle-solubilized spin-probe. The measured mobility ($1/\tau_{measured}$) of 16-doxylstearic acid methyl ester (16-DSE) is a combination of the mobility of the spin-probe within the micelle, with correlation time ($\tau_{relative}$), and the overall, much slower, tumbling of the micelle itself, characterized by ($\tau_{micelle}$). These two processes are independent and can be separated[10] by assuming that tumbling corresponds to the slowest motion of the micelle. $\tau_{micelle}$ may be calculated from the dimensions extracted from the SANS data using $R_{micelle} = X^{1/3}R_{core} + \delta_{shell}$;

$$\tau_{micelle} = \frac{4\pi\eta_{water}R_{micelle}^{3}}{3kT} \quad (3)$$

where η_{water} is the bulk viscosity of water. On the other hand, $\tau_{relative}$ is determined by the local dynamics and structure of the micelle;

$$\tau_{relative} = \frac{4\pi\eta_{local}R_{probe}^{3}}{3kT} \quad (4)$$

η_{local} corresponds to a local viscosity and R_{probe} is the effective hydrodynamic radius of the spin-probe. For 16-DSE, a value for R_{probe} of 3.75 Å has been used (see ref 10 for an extensive validation of this point). The local viscosity (η_{local}) experienced by the spin-probe is shown in Figure 3 as a function of x_{SDS}

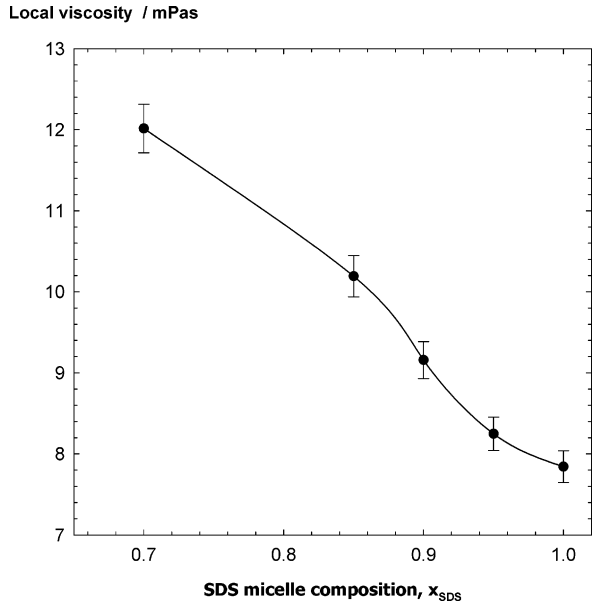

Figure 3. Local viscosity of the micelle headgroup region calculated from the rotational correlation time of the spin-probe 16-DSE for mixed micelles comprising sodium dodecylsulfate SDS and $C_{12}E_4$ as a function of micelle composition x_{SDS}.

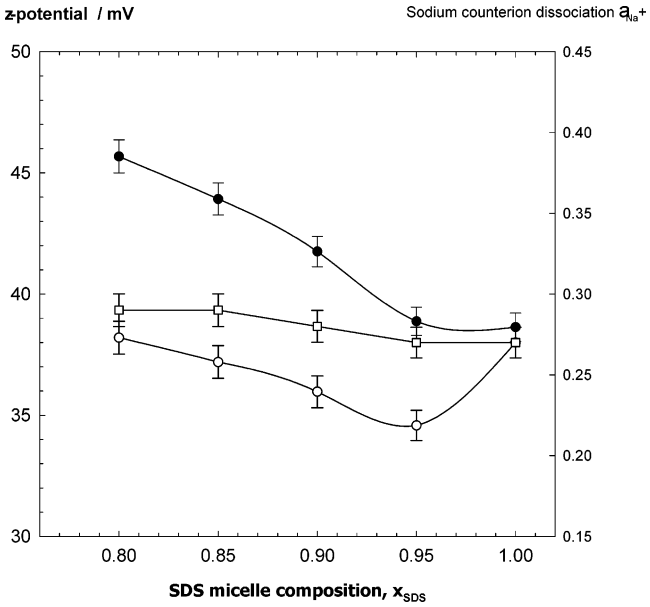

Figure 4. ζ-potential (●) calculated from the large particle limit for mixed micelles calculated from the electrophoretic mobility for mixed micelles comprising sodium dodecylsulfate SDS and $C_{12}E_4$ as a function of micelle composition x_{SDS}. Also shown are the degree of sodium counterion dissociation calculated from these ζ-potentials (○) and that extracted from the SANS analysis (□).

and ranges from 7 to 12 mPas. For reference, ethylene glycol has a bulk viscosity of 16 mPa s, 1-decanol 11 mPa s, and water 0.89 mPa s. With decreasing SDS mole fraction, the local viscosity increases due to steric hindrance between the bulky nonionic headgroups. As water is "squeezed out" of the headgroup region there is a concomitant decrease in mobility of the spin-probe. A similar change in local viscosity was reported by Moises.[15]

Hence, combining the EPR, TRFQ, and SANS techniques allows us to build a more detailed picture of the different regions of the micelle than is possible within any of these techniques individually. In principle, all of this information *is* contained within the SANS data but it is not possible to elucidate the detail with any degree of certainty without constraining the model. The SANS data do, however, contain further information relating to the ionic character of the micelle, and extracting this information is dependent on how we parametrize the structure factor. Traditionally, the parameters describing the $S(Q)$ (hard-sphere radius and volume fraction, micellar charge, and Debye length (ionic strength)) are constrained by assuming that the hard-sphere radius is consistent with the dimensions extracted from the form factor $P(Q)$ and that the hard-sphere volume fraction is equally accessible given the known concentration. The Debye length and micellar charge are coupled, as any dissociated counterion contributes to the ionic strength.

We have adopted the simplest approach in which the hard-sphere radius and micelle charge were allowed to float in the fitting but the Debye length and surfactant volume fraction were constrained. The Debye lengths were calculated by assuming a constant value $\alpha_{Na^+} = 0.27$. From the fitted charge (Table 1), α_{Na^+} can be recalculated (postfitting) and was found to lie within experimental error (~10%) of the assumed constant value $\alpha_{Na^+} = 0.27$. Similarly, the fitted hard-sphere radii were (within a similar experimental error) comparable to an appropriate effective spherical dimension.

However, an independent estimate of the ionic character of the mixed micelle may be obtained from electrophoretic NMR measurements. Within the large particle limit,[34] $u_\pm = \epsilon_o\epsilon_e\zeta/\eta$, the electrophoretic mobility may be converted to the ζ-potential of the micelle, and ultimately, to a relative degree of counterion binding, $\alpha_{Na^+}^{\text{mixed micelle}}$ within the mixed micelle. To do this, we need to understand how the micelle mobility evolves with composition, aggregation number, and morphology

$$u_\pm^{\text{mixed micelle}} \propto \frac{\alpha_{Na^+}^{\text{mixed micelle}} x_{SDS} N_{agg}^{\text{mixed micelle}}}{6\pi\eta\left(\frac{3N_{agg}^{\text{mixed micelle}} V_{\text{dodecyl}}^{\text{tail}}}{4\pi}\right)^{1/3}} \quad (5)$$

where $\alpha_{Na^+}^{\text{pureSDSmicelle}} = 0.27$ and hence

$$\frac{u_\pm^{\text{mixed micelle}}}{u_\pm^{\text{pureSDSmicelle}}} = \frac{\alpha_{Na^+}^{\text{mixed micelle}}}{\alpha_{Na^+}^{\text{pureSDSmicelle}}} \quad (6)$$

These data are shown in Figure 4. With increasing nonionic mole fraction, the ζ-potential **increases** slowly at first, then more rapidly.[44] Associated with an increase in the nonionic composition is micelle growth. Therefore, there is a concomitant increase in the number of ionic species present within the micelle and, hence, charge. On the other hand, α_{Na^+} is largely invariant, in excellent agreement with the conductivity studies of Iglesis and Montenegro,[16] reflecting the rather complex interplay of α_{Na+}, the aggregation number, and x_{SDS}. Also shown is the SANS derived estimate of the same quantity, and the agreement is surprisingly good within the experimental error.

We conclude that as SDS molecules present in the micelle are replaced by $C_{12}E_m$, the polarity and hydration of the headgroup region decreases, in agreement with other studies, but that there is no significant change in the overall degree of sodium counterion binding. However, for other poly(ethoxylated) surfactants with a greater number of ethylene oxide units[45−47] and for dimethylphosphine and dimethylamine,[48] a decrease in counterion binding is generally observed due to the decreasing surface charge density as the headgroup of the ionic surfactant is diluted over the micelle surface. For short chain ethoxylated surfactants[16,18] and our previous work on SDS/sugar

surfactants,[13] no significant change is observed in the counterion binding, at least over the composition range that is rich in ionic surfactant, $x_{SDS} > 0.8$, in agreement with the theoretical predictions of Hall et al.[47] and Maeda et al.[48]

Recently, Srinivasan and Blankschtein[5] have modified their molecular−thermodynamic theory to consider the effects of counterion binding on the micellization of (simple) ionic surfactants. Their calculations show that as the curvature of the micelle decreases (i.e., an increasing aggregation number), the degree of counterion binding increases (i.e., the degree of counterion dissociation decreases). Thus, two competing factors can be present in mixed surfactant micelles dependent on how the micelle morphology responds to changes in composition. For mixed surfactant micelles where there is little change in aggregation number and therefore micelle curvature, the effect of the nonionic surfactant is simply to dilute the surface charge and, hence, the degree of counterion dissociation simply increases. When there is an increase in aggregation number as the nonionic is added, reflecting a more rodlike micelle, the decreasing curvature of the micelle will result in a decrease in the degree of counterion dissociation. Given a sufficiently diluted ionic surfactant micelle, the counterion dissociation will subsequently increase with increasing nonionic micelle mole fraction. This simple approach may account for the weak minimum in the observed counterion binding (Figure 4) and the distinction between the various ethoxylated surfactants, but more data are required to clarify this issue.

We further show therefore that ENMR can be combined with TRFQ and EPR to assist in the fitting of SANS data and the agreement between these four quite different techniques lends considerable support to the validity of each experimental approach.

Conclusions

SANS, ENMR, TRFQ, and EPR have been used to study the structure of mixed anionic/nonionic surfactant micelles of SDS/$C_{12}E_4$. An elliptical core−shell morphology was found to describe the SANS data in which the core volume and shell thickness were defined on the basis of the TRFQ and EPR results, respectively, in conjunction with known values of the respective headgroup volumes. ENMR was shown to provide an independent measurement of the charge on the micelle, to further verify the SANS fitting.

With decreasing x_{SDS}, the local viscosity of the headgroup region increases due to the combined effects of more bulky nonionic headgroups and a reduction in the amount of water present in the headgroup region. We have therefore shown that combining EPR, ENMR, TRFQ, and SANS affords a greater insight into the headgroup region of surfactant micelles, yielding information that is otherwise difficult to extracted from any one technique alone.

Acknowledgment. P.C.G. and A.P. acknowledge the financial support of the Leverhulme Trust. P.S. thanks NFR (the now discontinued Swedish Natural Science Research Council) and its successor VR (The Swedish Research Council).

References and Notes

(1) Abe, M.; Ogino, K. Mixed Surfactant Systems. In *Solution Properties of Anionic−Nonionic Mixed Surfactant Systems*; Schick, M. J., Fowkes, F. M., Eds.; Surfactant Science Series; Dekker: New York, 1997

(2) Clint, J. *J. Chem. Soc.* **1975**, *71*, 1327.

(3) Rubingh, D. N. *Solution Chemistry of Surfactants*; Plenum Press: New York, 1979.

(4) Blankschtein, D.; Shiloach, A.; Zoeller, N. *Current Opin. Colloid Interface Sci*. **1997**, *2*, 294. Sarmoria, C. Puvvada, S.; Blankschtein, D. *Langmuir* **1992**, *8*, 2690.

(5) Srinivasan, V.; Blankschtein, D. *Langmuir* **2003**, *19*, 9932, 9946.

(6) Bergstrom, M.; Eriksson, J. C. *Langmuir* **2000**, *16*, 7173. Bergstrom, M. *Langmuir* **2001**, *17*, 993.

(7) Penfold, J. *Encyclopedia of Surface and Colloid Science*;Marcel Dekker: New York, 2002; p 3653.

(8) Pedersen, J. S. *Current Opin. Colloid Interface Sci*. **1999**, *4*, 190.

(9) Griffiths, P. C.; Roe, J. A.; Jenkins, R. L.; Reeve, J.; Cheung, A. Y. F.; Hall, D.G.; Pitt, A.R.; Howe, A.M. *Langmuir* **2000**, *16*, 9983.

(10) Bales, B. L.; Ranganathan, R.; Griffiths, P. C. *J. Phys. Chem. B* **2001**, *105*, 7465.

(11) Griffiths, P. C.; Whatton, M. L.; Kwan, W.; Abbott, R. J.; Pitt, A. R.; Howe, A. M.; King, S. M.; Heenan, R. K. *J. Colloid Interface Sci.* **1999**, *215*, 114.

(12) Griffiths, P. C.; Bales, B. L.; Howe, A. M.; Pitt, A. R.; Roe, J. A. *J. Phys. Chem. B* **2000**, *104*, 264.

(13) Griffiths, P. C.; Pettersson, E.; Stilbs, P.; Cheung, A. Y. F.; Howe, A. M.; Pitt, A. R. *Langmuir* **2001**, *17*, 7178.

(14) Griffiths, P. C.; Stilbs, P.; Paulsen, K.; Howe, A. M.; Pitt, A. R. *J. Phys. Chem. B* **1997**, *101*, 915.

(15) Moises de Oliveira, H. P.; Gehlen, M. H. *Langmuir* **2002**, *18*, 3792.

(16) Iglesis, E.; Montenegro, L. *Phys. Chem. Chem. Phys.* **1999**, *1*, 4865.

(17) Penfold, J.; Staples, E.; Thompson, L.; Tucker, I.; Hines, J.; Thomas, R. K.; Lu, J. R.; Warren, N. *J. Phys. Chem. B* **1999**, *103*, 5204.

(18) Penfold, J.; Staples, E.; Tucker, I. *J. Phys. Chem.* **2002**, *106*, 8891.

(19) Douglas, C. B.; Kaler, E. W. *Langmuir* **1994**, *10*, 1075.

(20) Shiloach, A.; Blankschtein, D. *Langmuir* **1998**, *14*, 7167.

(21) Feitosu, E.; Brown, W. *Langmuir* **1998**, *14*, 4460.

(22) Davidson, C. J. Ph.D. Thesis, University of Aberdeen, 1983.

(23) Gehlen, M. H.; De Schryver, F. C. *Chem. Rev.* **1993**, *93*, 199.

(24) Infelta, P. P.; Grätzel, M.; Thomas, J. K. *J. Phys. Chem.* **1974**, *78*, 190.

(25) Tachiya, M. *Chem. Phys. Lett*. **1975**, *33*, 289.

(26) Ranganathan, R.; Tran. L. Bales, B. L. *J. Phys. Chem*. **2000**, *104*, 2260.

(27) Hayter, J. B.; Penfold, J. *Colloid Polym. Sci.* **1983**, *261*, 1851.

(28) Bales, B. L.; Messina, L.; Vidal, A.; Peric, M.; Nascimento, O. R. *J. Phys. Chem. B* **1998**, *102*, 10347.

(29) Hayter, J. B.; Penfold, J. *Mol. Phys.* **1981**, *42*, 109.

(30) Griffiths, P. C.; Paul, A.; Penfold, J.; Ranganathan, R.; Bales, B. L. *Langmuir*, submitted for publication.

(31) Bales, B. L. Inhomogeneously Broadened Spin-Label Spectra; In *Biological Magnetic Resonance*; Berliner, L. J., Reuben, J., Eds.; Plenum Publishing Corp.: New York, 1989; Vol. 8, p 77.

(32) Bales, B. L.; Stenland, C. *J. Phys. Chem*. **1993**, *97*, 3418.

(33) Holz, M.; Müller, C. *Ber. Bunsen-Ges. Phys. Chem.* **1982**, *86*, 141.

(34) Holz, M. *Chem. Soc. Rev.* **1994**, *23*, 165.

(35) Johnson, C. S., Jr. Electrophoretic NMR. *Encyclopedia of Nuclear Magnetic Resonance*; Wiley & Sons: New York, 1996 (see also references therein).

(36) Saarinen, T. R.; Johnson, C. S., Jr. *J. Am. Chem. Soc*. **1988**, *110*, 3332.

(37) Johnson, C. S., Jr.; He, Q. Electrophoretic NMR. In *Advances in Magnetic Resonance*; Warren, W. S., Ed.; Academic Press: San Diego, 1989; pp 133−133.

(38) He, Q. H.; Liu, Y. M.; Sun, H. H.; Li, E. C. *J. Magn. Reson*. **1999**, *141*, 355.

(39) He, Q. H.; Lin, W.; Liu, Y. M.; Li, E. C. *J. Magn. Reson*. **2000**, *147*, 361.

(40) Hjertén, S. *J. Chromatogr*. **1985**, *347*, 1991.

(41) Griffiths, P. C.; Finney, G.; Cheung, A. Y. F.; Howe, A. M.; Pitt, A. R.; King, S. M.; Heenan, R. K.; Bales, B. L. *Langmuir* **2002**, *18*, 1065.

(42) Baglioni, P.; Dei, L.; Rivara-Minten, E.; Kevan, L. *J. Am. Chem. Soc.* **1993**, *115*, 4286.

(43) Ruiz, C. C.; Aguiar, J. *Mol. Phys.* **1999**, *97*, 1095.

(44) Griffiths, P. C.; Paul, A.; Stilbs, P.; Pettersson, E. *Langmuir* **2003**, *19*, 8605.

(45) Rathman, J. F.; Scamehorn, J. F. *J. Phys. Chem.* **1984**, *88*, 5807.

(46) Meguro, K.; Akusu, H.; Veno, M. *J. Am. Chem. Soc.* **1976**, *53*, 145.

(47) Meyer, M.; Sepulvbeda, L. *J. Colloid Interface Sci.* **1984**, *99*, 536.

(48) Rathman, J. F.; Scamehorn, J. F. *Langmuir* **1987**, *3*, 372.

(49) Hall, D. G.; Price, T. J. *J. Chem. Soc., Faraday Trans.* **1984**, *80*, 1193.

(50) Maeda, H. *J. Colloid Interface Sci*. **2003**, *258*, 390.